Portable multi-sensor air quality monitoring platform for personal exposure studies

Pelumi W. Oluwasanya, Abdullah Alzahrani, Varindra Kumar, Yarjan Abdul Samad and Luigi G. Occhipinti

***Abstract*—Poor air quality is known to cause different health issues both for short- and long-term exposure. Regulating organizations such as WHO, DEFRA, and EPA have specified acceptable limits of exposure to the main pollutants present in air. Portable multi-sensor devices are needed, with high accuracy and selectivity to multiple polluting and toxic agents present in air, to allow high spatial and temporal resolution in personal exposure monitoring. When compared to large centralized air quality monitoring centres, portable multi-sensor devices for air quality monitoring allow individuals to monitor their personal exposure levels in real time and cost-effectively. Environmental sensors are adopted in smart buildings, cars and gradually being integrated in portable form factor, for ambient air quality monitoring. We propose a non-intrusive air quality monitoring platform capable of sensing multiple gases and particulate matter, suitable for personal exposure monitoring and studies. The same platform integrates capabilities and bespoke front-end electronics for both capacitive and resistive sensors, with high accuracy and versatility. To demonstrate the significance of the proposed platform we report here the results of both simulations and measurements in monitoring $PM_{2.5}$, PM_{10} and NO_2 as an example of capabilities toward the overarching goal of covering the entire spectrum of air pollutants, and to integrate it into smart portable devices.**

***Index Terms*—Air Quality, Gas sensing, Printable sensors, Personal Exposure Monitoring, $PM_{2.5}$, PM_{10}, Air pollution, Environmental sensors**

I. Introduction

Poor air quality is considered among the main causes for millions of premature deaths annually, about 8 million in 2012 according to the World Health Organization [1]. Several epidemiological studies have found a relationship between exposure beyond specified limits and burden of disease [2].These and many more have led to an increased and urgent need to both monitor and

Submitted 3rd March 2019. This work was supported in part by InnovateUK (GraphClean G.A. No. 71476-481865), EPSRC Sensors CDT (G.A. No. EP/KO3099X/1), EPSRC CIMLAE (G.A. No. EP/LO15889/1) and the Presidential Special Scholarship for Innovation and Development (PRESSID) managed by the National Universities Commission (NUC) and funded by the Petroleum Technology Development Fund (PTDF).

Pelumi W. Oluwasanya is a PhD student in Electrical Engineering Division, University of Cambridge Department of Engineering, 9 JJ Thomson Avenue, Cambridge CB3 0FA.

Abdullah Alzahrani is a Postdoctoral researcher at the Electrical Engineering Division, University of Cambridge Department of Engineering, 9 JJ Thomson Avenue, Cambridge CB3 0FA.

Varindra Kumar is a Postdoctoral researcher at the Electrical Engineering Division, University of Cambridge Department of Engineering, 9 JJ Thomson Avenue, Cambridge CB3 0FA.

Yarjan Abdul Samad is a Postdoctoral researcher of the Cambridge Graphene Centre, Department of Engineering, University of Cambridge, 9 JJ Thomson Avenue, Cambridge CB3 0FA.

Luigi G. Occhipinti is Director of Research at Department of Engineering, University of Cambridge, 9 JJ Thomson Avenue, Cambridge CB3 0FA. Phone: +44 7548 323462, Email: luigi.occhipinti@eng.cam.ac.uk (corresponding author)

consequently limit personal exposure to harmful pollutants [3]. There is a generalized attention from different governmental agencies globally to limit anthropogenic emissions via legislations and policies. City councils, including for instance in Cambridge, UK, promote new policies that help accelerate switching from combustion engines to electric vehicles both for public and for private transport, accompanied by installation of a distributed urban network of rapid charging points by 2020 [4], along with imposition of road taxes, and exemption from the same based on vehicles emission of polluting gases and smaller particulate matter ($PM_{2.5}$). Besides, reduction of indoor wood burning for heating, as one of the largest sources of indoor particulate matter, also has the potential to drastically reduce $PM_{2.5}$ exposure levels. Citizens are nowadays more conscious and attentive of their personal exposure to polluting agents and environments, and prone to adopt cleaner solutions for living, transport, energy generation and heating. Adoption of personal exposure monitoring devices on an individual level therefore offers multiple benefits and is motivated by the willingness to continue making healthier choices in everyday life consistently. Access to high resolution data of personal exposure with high space and time accuracy is however difficult to achieve with currently available centralized or public network of monitoring stations. Providing individuals with portable devices for air quality monitoring that operate in real time and allow them to monitor and record their personalized exposure levels in combination with conventional geolocation offering a half-meter or less space resolution, may become a unique instrument and breakthrough not only for the individuals, but also for the city councils, and other government agencies to shape and fine-tune their policies for control of air quality in urban, industrial and rural areas. This is possible with use of both existing and emerging technologies for autonomous sensors, data communication and modern mobile networks, including Internet of Things.

The first implication of this is that the sensor platform must be non-intrusive, integrated in objects of everyday use and environments, such as in cars, bikes, or in offices and homes, and possibly combined or communicating with other portable devices of everyday use, e.g. smartphones, tablets and laptops. Another implication is that the platform should monitor as many pollutants as possible at the same time and able to both inform the user in real time and to record these data in datalog files for later use. This has proven to be a challenge for most of the currently demonstrated sensors and integrated platforms, due the rapid increase in size and complexity of both the hardware and software instruments needed to operate different technologies.

Here we propose a multi-sensor platform that has the potential to achieve the necessary level of functionality and integration, as needed to provide the user with easy access to the relevant data at any time. A clear benefit and future evolution of the proposed platform consists of the possibility to incorporate machine learning algorithms and artificial intelligence tools in the system that makes it personalized to the user's habits, by learning individual activities and location and correlating these with measured data. This may allow the user to take informed decisions that limit exposure to potentially dangerous agents. Through integration with smartphones, it may be possibly to access information about known relationships between exposure to such agents and likelihood of disease and use these to provide the user with options for safer routes and activities, creating a history of individual personal exposure for better understanding of personalized health monitoring over time.

To demonstrate the significance of the proposed platform, without limiting the range of functionalities for a comprehensive monitoring of all possible polluting and toxic agents present in air, we focused here on monitoring Particulate Matter (PM) of sizes smaller than 10 microns and 2.5 microns in aerodynamic diameter (PM_{10} and $PM_{2.5}$ respectively), and Nitrogen Dioxide (NO_2). We report the design, simulation and implementation of both sensors and the possibility of their integration into a single platform.

II. MULTI-SENSOR PLATFORM DESIGN AND FABRICATION

The multi-sensor platform comprises an array of interdigitated electrodes that have been functionalized with active sensing materials that make them sensitive and selective to specific analyte. The platform comprises miniaturized dual housing for gas

sensors and PM sensors as shown in Figure 1a. Sampled air enters the PM detection chamber first where a temperature gradient due to the heater near the inlet is used to separate the entrained particles into different streams based on their sizes. These are detected on the sensors arranged perpendicularly to the flow to intercept it. The effects of temperature can be removed by collocating a temperature sensor with the measurement electrodes. Measurement noise is removed by using a differential approach. Air leaves this PM detection chamber via an outlet which doubles as an inlet for the gas detection chamber in which sensors are arranged as shown to detect different gases before exiting the chamber finally. The height of the chamber is of the order of 1cm. These sensors are fabricated on a flexible substrate using conventional lithography. The platform is shown in Figure 1a. The different parts of the device are now presented with a brief background in each case.

III. $PM_{2.5}$ Detection

Airborne particulate matter, whether indoor or outdoor is harmful to health. PM_{10} is regarded as less harmful as it can be sneezed out when inhaled. $PM_{2.5}$ however can cross the tissue-blood barrier potentially causing harm depending on its chemical constituents. For this reason, human PM exposure limits have been set by regulatory bodies such as the Environmental Protection Agency (EPA) and World Health Organization (WHO). However, the concentration levels of both large and small PM in metropolitan and industrial areas and regions worldwide, for example China, might exceed the safe limits at times, in association with high level of emission or environmental conditions locally, with detrimental effects for the health of inhabitants [5]. This remains a challenge to deal with in many of such areas. Policies to reduce the ambient PM levels in these areas must depend on sources present locally in each area, throughout days and nights for an entire year, to be effective and efficient in capturing actual cycles, environmental influences and habits of inhabitants. For instance, there is evidence that ambient PM concentration levels are influenced by wind. Migration of PM emitted from location to location due to wind has shown that the danger posed is not related to the source's immediate environment only [6].

With reduction in PM sizes also comes increasing persistence in ambient breathable air as gravity becomes too small to effect natural particle deposition. Thus, smaller particles ($PM_{2.5}$) tend to stay longer in the outdoor air, and even more in buildings, vehicles and other enclosed spaces where dispersion is slower. In big buildings there are vents that allow for exchange of air at specific times of the day, but this is not guaranteed to ensure cleaner air without some filtering stage if the outdoor air is not cleaner than the indoor air, as can be the case in buildings near heavy traffic roads during the morning 'rush hour'.

PM collected from any ambient airflow has constituents which depend on the location being sampled. The composition of these particles can be organic or inorganic, and ranging from sulphates to carbon, nitrates, ions and radicals. There are differences in composition for different particle sizes and particle discrimination is needed in such studies, along with the study of Total

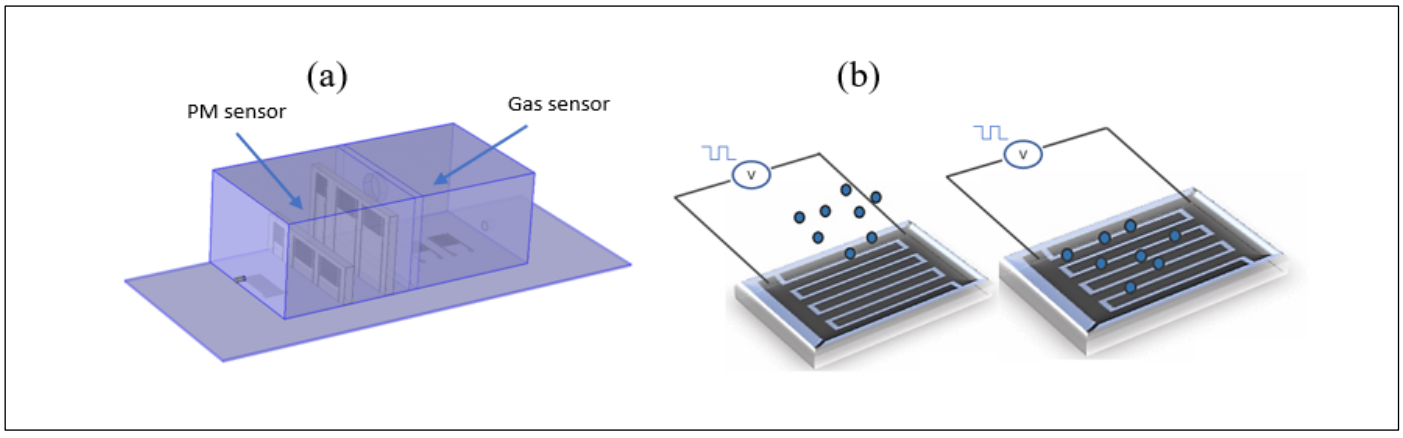

Figure 1 – (a) CAD of the multi-sensor platform showing the housing system and arrangement of the PM sensor and gas sensor blocks, respectively (left) (b) working principle of the capacitive PM detection device (right)

Suspended Particles (TSP). Thus, particle discrimination stages are usually quite an important part of all systems for PM monitoring, followed by the detection stage for each particle size.

$PM_{2.5}$ detection has been carried with a variety of methods and have been hugely successful in determining the particle mass concentration, number concentration and size distribution. However, $PM_{2.5}$ sensing devices have been generally difficult to miniaturize compared with gas sensor devices which have been miniaturized with success. It is not immediately clear how to miniaturize, for example a bulky gravimetric PM sensor and keep its sensitivity and accuracy. The most successful methods used instead for small sensors is light scattering-based. These small sensors have a cut-off point beyond which they cannot detect smaller particles, may demonstrate unit-to-unit deviation and are therefore less accurate than the traditional ones [7].

Hence, the most accurate PM detectors are housed in the air quality monitoring centers, which are present in countries in a limited number only, for instance the U.K. has around 300 centers. These PM detectors are usually gravimetric detectors which determine the PM mass concentration from the difference in the weight of the filter collector before and after the deposition of particles on it. Some gravimetric sensors are online and can provide real-time measurement. An example is the Tapered Element Oscillating Microbalance (TEOM) used for PM monitoring. It comprises a tapered tube with one fixed end and an oscillating end. The oscillating end attached to a filter collects particles which alters the frequency of oscillation. This leads to a direct PM mass concentration determination in real-time [8].

Light based techniques are divided into three broad categories which are absorption, scattering and extinction. PM detection via light absorption is used for measuring black carbon (BC) concentration because of its good light absorption property. Amaral *et al.*'s review [9] identified spot meter, aethalometer, photoacoustic soot sensor (PASS), and laser induced incandescence (LII) as examples of devices in this category. The spot meter, which is used in exhausts, measures the particle concentration of particles via the comparison of light reflected from opaque particle-laden filter and a baseline filter. Aethalometers are based on the attenuation of light of different wavelengths transmitted through a particle-laden filter. PASS involves detecting acoustic pressure waves that are generated from heat released by light-absorbing particles to surrounding air. LII measures incandescence intensity when heated particles reach incandescence. This, with decomposition rate provides metric for PM detection. Light scattering methods rely on the scattering of light (from lasers or LEDs) by particles flowing across its path. Scattered light is collected and then analyzed through an autocorrelation function usually of a short time lasting signal to obtain size distributions/average size as in the case of the ensemble detectors such as photometers or number concentration or volume concentration distribution as in the case of single particle detectors such as the Optical Particle Counter (OPC).

Impedance based methods have been demonstrated in the past and are still being used in several forms. They are usually based on depositing PM on substrates and then measuring the resistance/impedance of the material via a metal plate using probe stations or lock-in amplifier for frequency measurements for example in capacitive sensors [10]. Carminati *et al.*'s [10] capacitive PM_{10} sensor detected polystyrene beads of 10μm diameter (PM_{10}) and 8μm talc powder. Bianchi *et al.*, [11] presents an impedance-based particle detection technique where interdigitated microelectrodes, formed into fingers of pillar shape are arranged normal to the flow and as a particle passes in-between the electrodes, the impedance change is measured. Limitation of impedance-based techniques in $PM_{2.5}$ detection is the very low amplitude of the signals obtained for particles of that size hence their use for particles of larger size. Usability of this technique for particles of smaller size, as shown in this work, therefore requires both discrimination of smaller particles from larger ones present in the air flow and a highly accurate electronic readout circuitry.

Acoustic based particle sensors on the other hand rely on the frequency shift that occurs when a particle is deposited on an oscillating cantilever or element as a result of the increase in mass of the oscillating component. They are usually very sensitive devices. They rely on the Sauerbery equation for their analysis. Apart from mass and number concentration, some sensors provide size distribution output information. This is useful for ensemble characteristics and may be based on different particle properties

such as geometrical size, aerodynamic size, electrical mobility, inertia, and optical properties [12].

In this work, capacitive detection technique was used, based on the principle that when particles come into the active volume space of charged electrodes they produce a change in the dielectric constant of the capacitor, and their concentration can be obtained by measuring the minute changes in the capacitance between the same electrodes [7], [13]. For that, particle-entrained airflow needs to be filtered to remove particles larger than 10 microns in diameter. We added a critical step to the technique, where the resulting flow is subjected to a temperature gradient determining a different path for larger and for smaller particles and therefore allows separation and discrimination between PM_{10} and $PM_{2.5}$ before they are deposited on separate pairs of capacitive electrodes.

The electronic readout for the small capacitance changes produced by the small particles impacting in the sensing electrodes is based on Irvine sensors California's MS3110 readout ASIC with schematics shown in Figure 2, including a picture of an evaluation board. A 5V air pump purchased from Thomas (by Gardener Denver) was used for the work setting and controlling the flow rate.

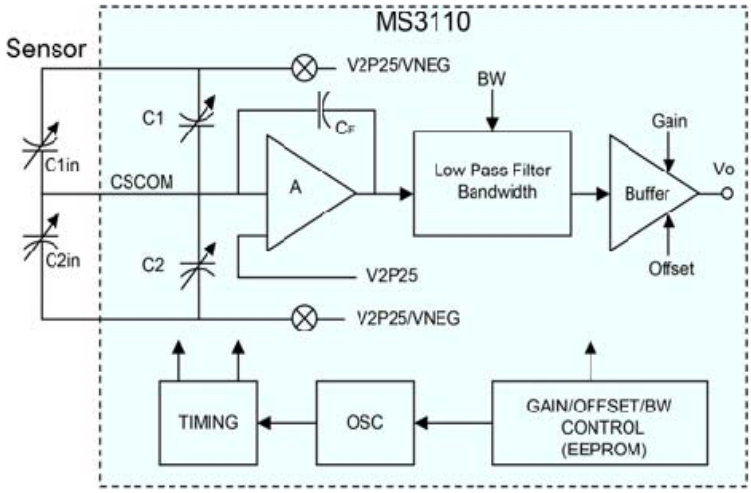

Figure 1 – Building blocks of the electronic readout circuit assembled on printed circuit board.

A. Sensor Fabrication and integration in the PM detection module

The PM_{10} and $PM_{2.5}$ sensors comprise a differential array of interdigitated electrodes arranged normal to the airflow, as shown in Figure 3 for a model prototype, and simultaneously detect both large and small size PM in the same airflow. Sampled air enters the PM detection chamber where a temperature gradient due to the heater near the inlet is used to separate the entrained particles into different streams based on their sizes. The arrangement of the sensors normal to airflow forces interception of the same, and resultant deposition on the electrode surface, causing step changes in capacitance as the relative permittivity of the active volume space above the electrode surface is increased by the presence of particles. The effects of temperature and parasitic capacitances are removed by using a differential approach, with control devices of the same size and arranged in the same chamber but passivated to not be subject of capacitance changes as effect of incident particles. The height of the chamber is of the order of 2 cm. These sensors are fabricated on a flexible substrate using conventional lithography.

AZ5214E image reversal photoresist was spin-coated for 40 seconds at 4000rpm on 50 micron-thick Kapton^{HN} purchased from

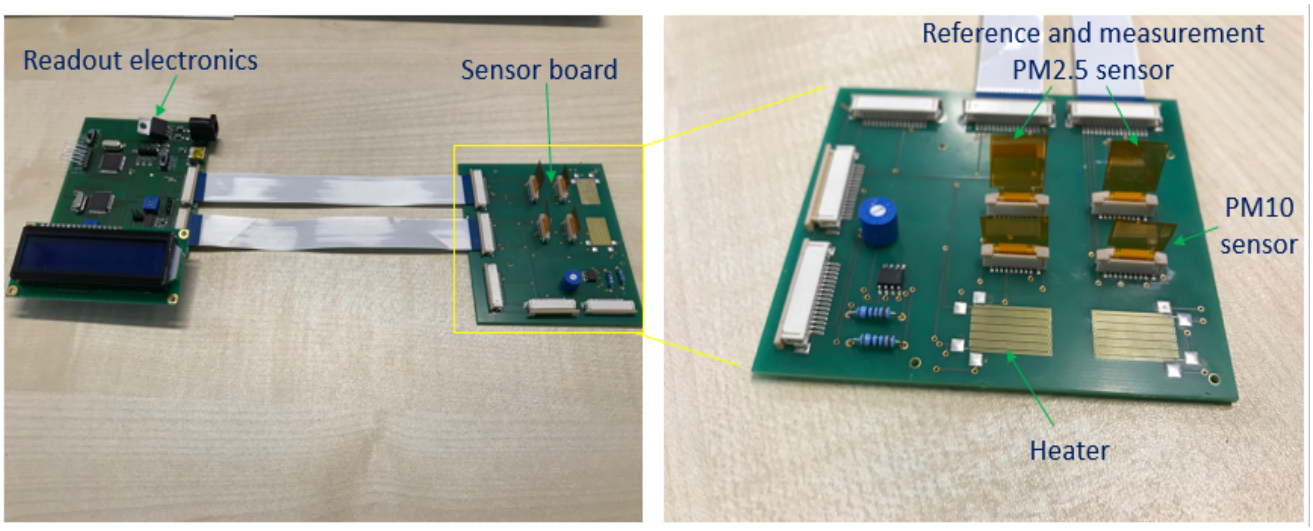

Figure 3 - Integration of the fabricated sensor and the printed circuit board.

a distributor of electronic materials (RS) and prebaked for one minute at 105°C. It was then patterned using a negative photomask using the MJB 4 contact mask aligner with exposure time of 8 seconds using soft contact and align & expose setting. This step is then followed by a post-exposure bake for 2 minutes at 120°C on a hotplate. A flood exposure was then carried out for 30 seconds. Development of the patterns was done using AZ351B mixture with water in ratio 1:4 respectively. The sample was then blow-dried with a Nitrogen gun. Titanium and Gold metal layers were then deposited in that order using a Lesker e-Beam evaporator with thicknesses of 5nm and 50nm for each metal layer respectively before lift-off in acetone.

B. Sensor Electronics

The MS3110 Universal Capacitive Readout IC chip produces a range of analogue output voltages based on a capacitive difference at its input and can be programmed by its internal registers to compensate for any imbalance in the external capacitance. Its functional block diagram is shown in Figure 2 (right).

Its transfer function is given by:

$$V_o = Gain \cdot V_{2P25} \cdot 1.14 \cdot \frac{C_{S2T} - C_{S1T}}{C_F} + V_{REF} \qquad (1)$$

Where:

Gain = 2 or 4 V/V

V_{2P25} = 2.25V DC

$C_{S1T} = C_{SIN1}$(external) + C_{S1}(internal),

$C_{S2T} = C_{SIN2}$(external) + C_{S2}(internal),

C_F is the output stage gain capacitance and V_{REF} is selectable 0.5/2.25V output offset voltage.

C_{SIN1} and C_{SIN2} input capacitances form a bridge with the C_{S1} and C_{S2} adjustable internal capacitances. This bridge is driven by a bipolar internal square wave signal. A programmable gain and low pass filter are also used to increase the signal and filter out any high frequency components from the output before the signal is finally fed into a buffer to produce the output voltage V_o. As a result, V_o is proportional to the difference of input capacitances. The complete integrated device is shown Figure 3 (left) showing electronic readout interface with LCD and the sensor board, while the fabricated electrodes are shown in Figure 4 for both the PM sensor (left) and the gas sensor (right). This approach (having the sensor board separate from the readout electronics) introduced

some parasitic capacitances due to the cables, traces and ZIF connectors which then lead to reduce the Signal-to-Noise Ratio (SNR) in the initial prototype.

Thus, another PCB has been designed with compact integration of both the sensor module and the read-out electronics within the same PCB, with minimal length of traces and connectors.

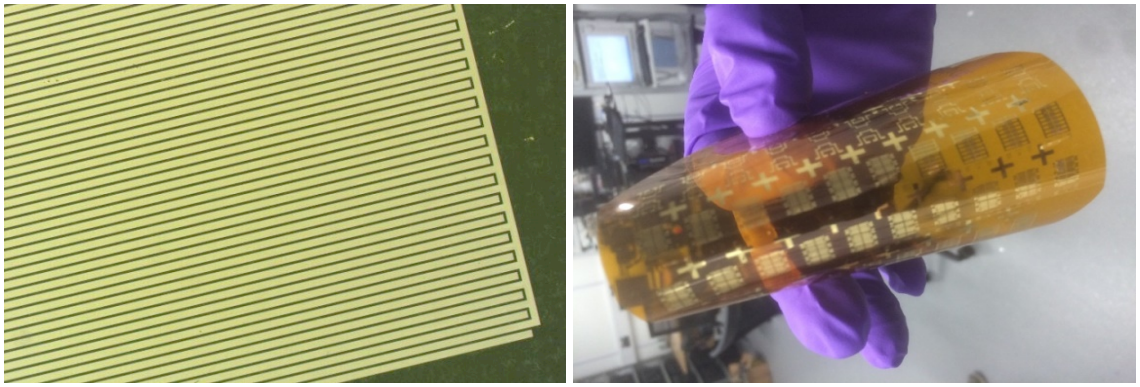

Figure 4 – Fabricated interdigitated PM sensor electrodes (left) and gas sensors (right).

IV. NITROGEN DIOXIDE DETECTION

NO_2 is an oxide of Nitrogen emitted from both natural and anthropogenic sources. The largest anthropogenic source of NO_2 is vehicular, from the burning of fossil fuels in the vehicle engines. Indoor cooking also contributes to short time peaks in ambient levels. Ambient levels of NO_2 are generally low, due to efforts of government and regulatory organization, and concentrations found in studies to cause respiratory problems generally are >1 ppm.

Metal oxide semiconductor, electrochemical and NDIR are different approaches that have been used in the past for NO_2 detection. One example is Yoshida *et al.* [14] using WO_3 which showed sensitivity to 2 ppm NO_2 but the process requires a high temperature (700°C) calcination process. Bott found that the best operational temperature for their NO_2 sensor was at 300°C [15], though the sensor could measure down to 1 ppb. To enable development of unheated metal-oxide based sensors, UV-sensitive metal oxides such as ZnO have also been utilized and the system provided with an UV LED to help accelerate the release of adsorbed gas molecules from the active sensing layer, therefore enabling successful room-temperature operation of the gas sensor [16]. In addition to this, selectivity to specific gas molecules, with reduced cross-sensitivity to interferent species is generally another challenge of metal oxide-based devices, hence the need for dopants [17]. More benefits can be obtained by combining these approaches in a single sensor device [18]. Further, with nanocomposite materials structures, sensitivity can be further enhanced thanks to the increase of the active surface area, and higher reactivity at the grain boundaries. This has led to the synthesis of nanocomposite structures based on highly conductive nanomaterials such as graphene, and a selective polymer binder material. The benefits of this include room temperature sensing achieved with materials that have been solution processed and can be deposited by drop-casting or printing.

For this work, a graphene-polymer composite was used as the sensing layer material. It was deposited on interdigitated electrodes by drop-casting in a trench using a syringe or a micropipette. Adsorption of the gas on the sensing layer causes a decrease in resistance of the material. Concentrations of NO_2 down to 20 ppm have been successfully measured in laboratory conditions.

A. Sensor Fabrication

The sensor array in this setup comprises an array of interdigitated electrodes that have been functionalized with active sensing materials that make them sensitive and selective to specific analyte, in this case NO_2. The fabrication technique for the interdigitated electrodes is similar to that already described. It allows for different active materials to be deposited on top of each set of electrodes in the array, for higher flexibility of the targeted application. This is further facilitated by a polymer bank technology, which allows to separate each set of electrodes in order to avoid cross-talk. The array of 8 polymer banks have been developed by depositing SU-8 2015 negative photoresist by spin-coating on the sample containing the interdigitated electrodes array and pre-bake it at 65°C for 1 minute before ramping up to 95°C for 3 minutes. A photomask was used to define the geometry of the polymer banks corresponding to active areas of the 8 electrodes in the array. The sample was then exposed to UV light for 11 seconds and developed in PGMEA for 3 minutes resulting in trenches opened on active areas that constitute the polymer banks. The prepared Graphene-Polymer ink for NO_2 sensing was then drop-casted into the trenches as shown in Figure 5.

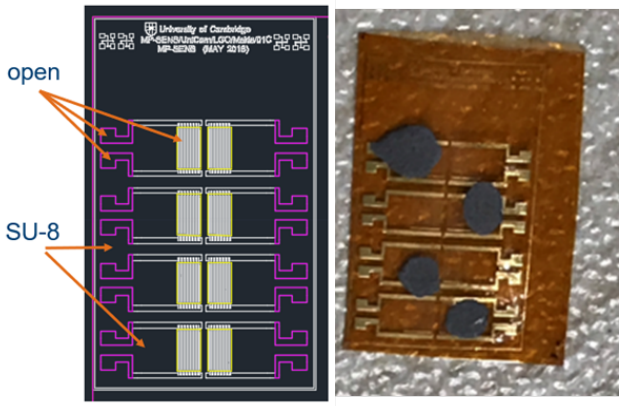

Figure 5 - CAD design and fabricated NO_2 sensor with Graphene-polymer composite drop-casted.

This was then dried on a hotplate at 80°C for 1 hour. The array of 8 pairs of interdigitated electrodes could be used for detection of up to 8 different analyte gases using corresponding sensing ink materials, or for increasing reliability of the measurements through up to 8 measurements or 4 differential measurements with 4 devices used as sensors and the remaining 4 as control. Moreover, to allow for easy integration with the readout electronics, the sensor was integrated with interposers which terminate in ZIF connectors contact for seamless fit into the slot of the printed circuit board.

B. Sensor Integration and Readout Electronics

Future sensor applications require custom solutions to sense and interact with the world. Printed electronic manufacturing method with hybrid integrated solution is a promising approach to both mass produce and customize sensor systems for different markets at low manufacturing costs and short lead time. The hybrid approach may include custom-made Printed Circuit Board (PCB) with an inhouse designed sensor. A low-cost flexible and miniaturized interposer PCB with the size 17 mm x 10 mm x 0.31 mm using foil on foil integration method has been designed to facilitate an easy and reliable integration of the x8 IDE sensor to the MCU based system through a sub-system holder. The PCB has been designed using DesignSpark and the result shown in Figure 6.

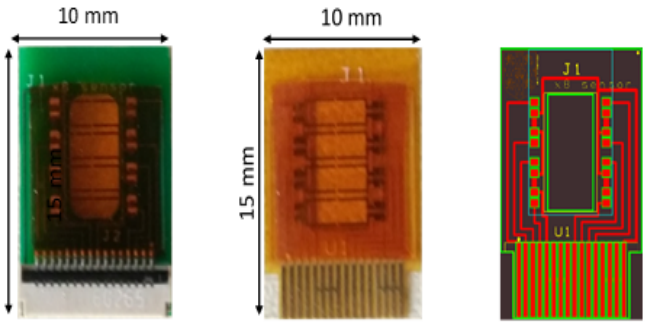

Figure 6 – Rigid PCB with IDE sensor (left), Flexible interposer with IDE sensor (middle), Interposer schematic (right)

To integrate the IDE sensor over the interposer PCBs a stencil was used to solder flexible sensor using the IR soldering equipment IR650A over interposer at low temperature, 140 ºC. The assembly equipment and the soldering profile used in the soldering is shown in Figure 7.

An Anisotropic Conductive Film (ACF 7376-10) was used to achieve the conductive adhesion between the pads of the sensor electrodes foil and the corresponding pads in the interposer foil, at high resolution and reliability. Good values of conductivity for the ACF bonding has been further assessed at higher temperature in the range of 150 ºC - 200 ºC.

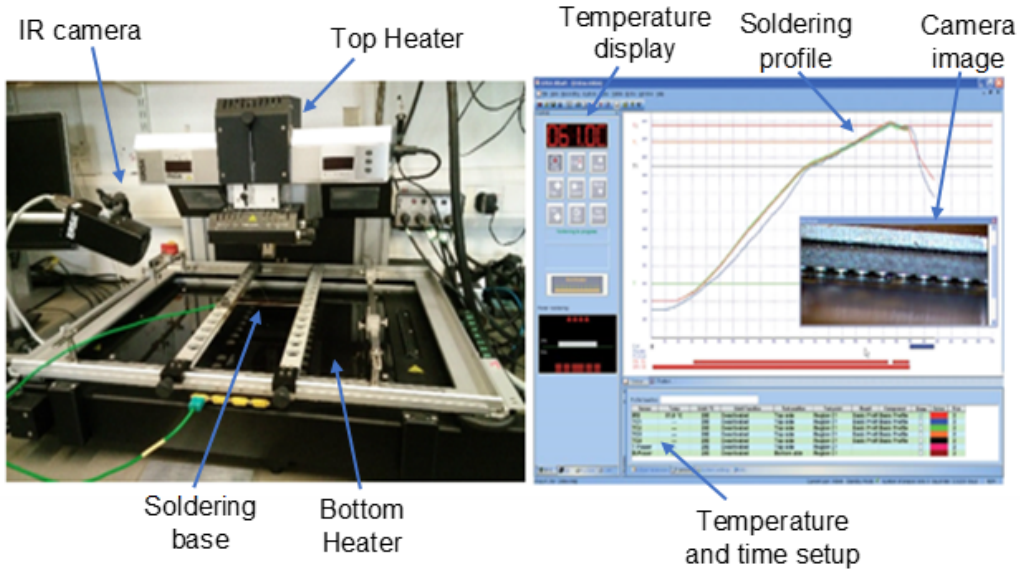

Figure 7 – IR 650A Assembly equipment(left), soldering profile of sensor and interposer ACF assembly (right)

The gas measurement is therefore based on the changes in electrical resistance of sensing electrodes and corresponding control devices connected in a Wheatstone bridge configuration, with balanced initial values in absence of polluting gases. The presence of targeted polluting gases is obtained from the changes between the value of electrical resistance measured in the IDE terminals against the corresponding reference values.

Finally, the system is provided with additional communication capabilities and standard protocol interfaces, to allow transfer of data in real time to portable devices, such as smartphones and tablets, and software for data transfer and representation with graphic

user interfaces. Figure 8 shows an example of a simple GUI for real time display and control of data acquisition by using HID USB/UART communication.

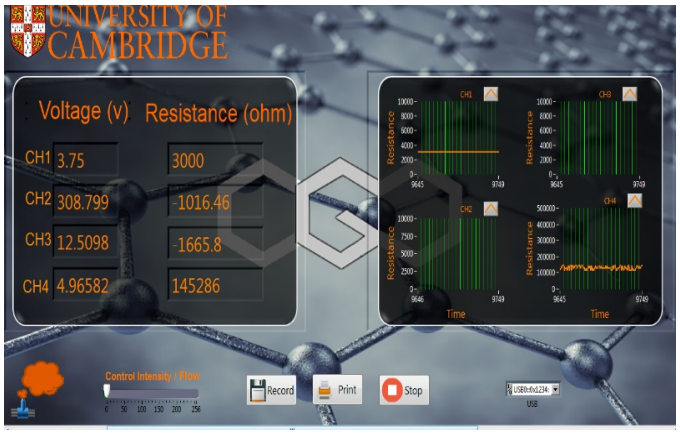

Figure 8 - Graphical User Interface (GUI) for real time display and data acquisition of the Gas sensor

V. RESULTS

The capacitive PM sensing capabilities were first verified via simulation using COMSOL finite element analysis tool. A summary, presented in Figure 9 (left) shows the capacitance changes as a single particle moves away from the surface of the electrodes for different horizontal positions for an electrode finger width of 10 microns and an inter-electrode spacing of 4 microns, and a particle size of 2 microns in aerodynamic diameter. From the figure, the highest capacitive changes occur at the surface of the electrodes when the particle is within the active volume space of the charged electrodes field. Further, the highest signal level for each of the measurement points is for the position (x = 12 microns) in-between the oppositely charged electrode fingers, as expected. Step changes of this can be expected for multiple particles of similar size range. A static measurement carried out shows a capacitive change when talc particles of 10um aerodynamic diameter were deposited using tweezers on the surface of the charged electrodes. This result is shown in Figure 9 (right), Given the larger size of the particles and larger number deposited with the tweezer, a step change of up to 25 fF was obtained as shown.

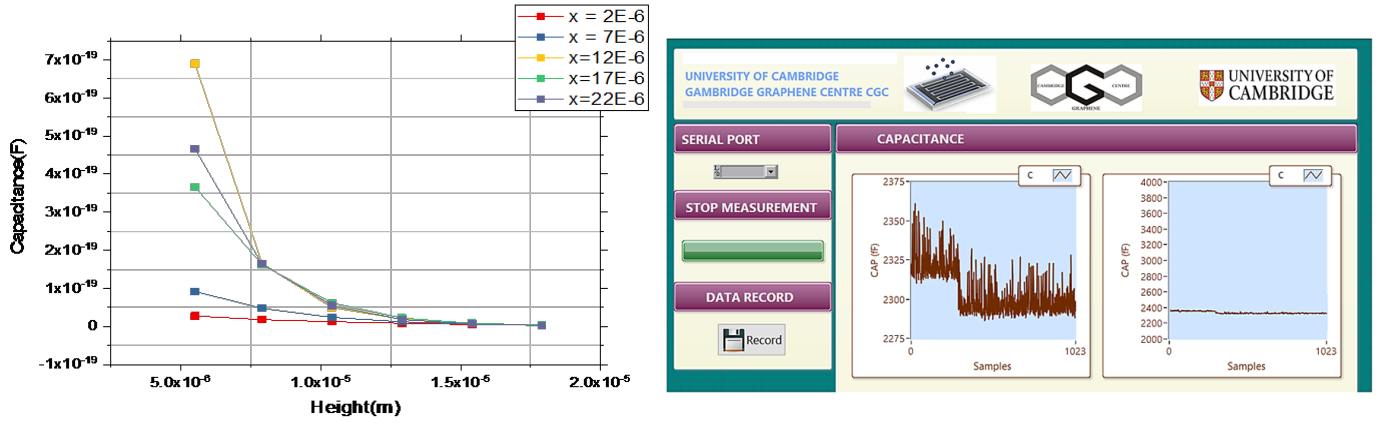

Figure 9 - Capacitive measurements for PM2.5 as a single particle moves from very close to the sensor surface (left) and actual experimental measurements when talc particles of PM10 are deposited on the sensor electrodes in a static test in the laboratory.

Preliminary measurements of sensor response to NO_2 is shown in Figure 9. The material was subjected to increasing concentrations of the analyte gases from 20 ppm to 80 ppm in increments of 20, except for CO_2, which was done from 20000 ppm to 80000 ppm in increments of 20000 as shown in Figure 10. In case of NO_2, clear step changes were observed as the concentration was increased from 0 ppm to 80 ppm in steps of 20. As the concentration approaches 80 ppm, the step changes reduce. This is after a much larger increase (20%) observed at 40 ppm. This can be an early sign of sensor saturation. At 80 ppm, the sensor saturates. The first response of the material, however, is around 15% to 20 ppm NO_2.

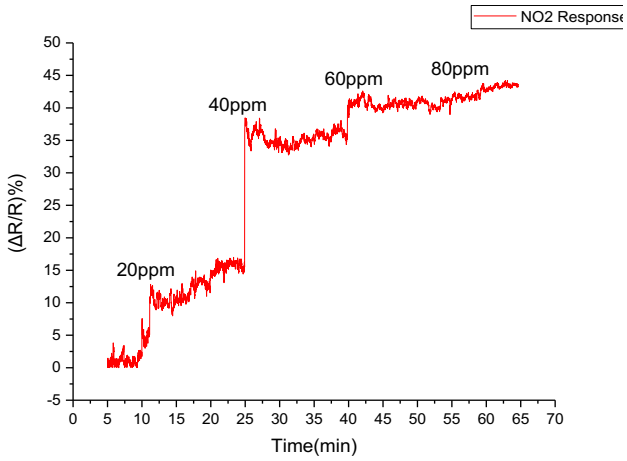

Figure 10 – Sensor response to NO_2 of increasing concentration

Selectivity was tested for successively exposing the material to other gases. These include Ammonia (NH_3) and Carbon dioxide (CO_2). The exposure was done in increasing concentration for the gases. The increment was 20ppm for ammonia and 20,000ppm for CO_2 each time. The sensor showed very little response to ammonia, not exceeding 5%, even at 80ppm. The material also showed no detectable response to CO_2.

A comparison of the sensor responses is shown in Figure 11, which shows that the sensor is selective to NO_2. Further sensitivity improvement of these sensors is needed, along with technical solutions to remove sensor saturation and to expand the pollution monitoring range.

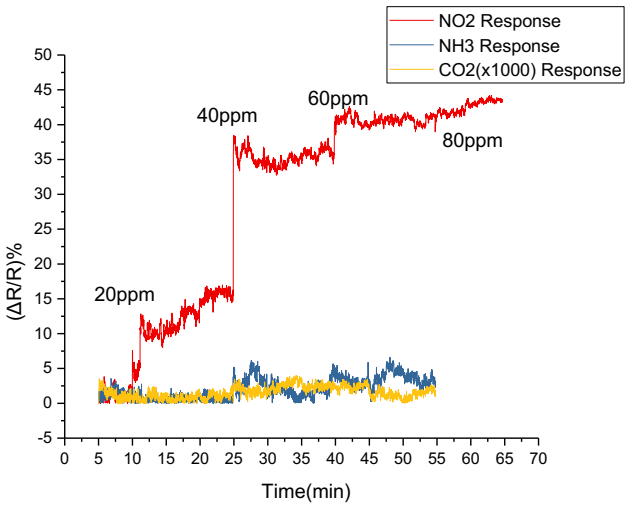

Figure 11 – Comparison of sensor response to increasing concentrations of NO_2, CO_2 and ammonia.

VI. Conclusion

A compact sensor platform for personal exposure monitoring has been presented. This includes a capacitive PM sensor, with an innovative feature of discrimination between $PM_{2.5}$ and PM_{10} based on thermophoresis, together with an array of resistive chemical sensors for monitoring multiple polluting agents present in air. The work is an example of an integrated multi-functional system for air quality monitoring suitable for integration in portable devices to help individuals make healthier choices in their daily activities and habits. Device architecture, front-end readout electronics and preliminary measurements have been reported as an example of integration of the different function block units and their working principles reported in details.

Acknowledgment

The authors would like to thank InnovateUK (GraphClean G.A. No. 71476-481865 and MP-SENS 73047-501268), EPSRC Sensors CDT (G.A. No. EP/KO3099X/1), EPSRC CIMLAE (G.A. No. EP/LO15889/1) and the Presidential Special Scholarship for Innovation and Development (PRESSID) managed by the National Universities Commission (NUC) and funded by the Petroleum Technology Development Fund (PTDF).

References

[1] World Health Organization, “Burden of disease from Household Air Pollution for 2012,” 2012.

[2] T. O. Etchie, S. Sivanesan, A. T. Etchie, G. O. Adewuyi, K. Krishnamurthi, K. V George, and P. S. Rao, “Chemosphere The burden of disease attributable to ambient PM2 . 5-bound PAHs exposure in Nagpur , India,” *Chemosphere*, vol. 204, pp. 277–289, 2018.

[3] L. G. Occhipinti and P. W. Oluwasanya, “Particulate Matter Monitoring : Past , Present and Future,” *Int. J. Earth Environ. Sci.*, vol. 2, no. 144, pp. 2–5, 2017.

[4] Cambrridge City Council, “Taxi drivers urged to consider switching vehicles as rapid electric charging points are launched,” 2018. [Online]. Available: https://www.cambridge.gov.uk/news/2018/10/03/taxi-drivers-urged-to-consider-switching-vehicles-as-rapid-electric-charging-points-are-launched.

[5] Y. Song, X. Wang, B. A. Maher, F. Li, C. Xu, X. Liu, X. Sun, and Z. Zhang, “The spatial-temporal characteristics and health impacts of ambient fine particulate matter in China,” *J. Clean. Prod.*, vol. 112, pp. 1312–1318, 2016.

[6] G. D. Thurston and J. D. Spengler, “A quantitative assessment of source contributions to inhalable particulate matter pollution in metropolitan Boston,” *Atmos. Environ.*, vol. 19, no. 1, pp. 9–25, 1985.

[7] R. M. Harrison and J. Yin, “Particulate matter in the atmosphere: Which particle properties are important for its effects on health?,” *Science of the Total Environment*. pp. 85–101, 2000.

[8] H. Patashnick and E. G. Rupprecht, “Continuous PM-10 Measurements Using the Tapered Element Oscillating Microbalance,” *J. Air Waste Manage. Assoc.*, vol. 41, no. 8, pp. 1079–1083, 1991.

[9] S. Simões Amaral, J. Andrade De Carvalho, M. A. Martins Costa, and C. Pinheiro, “An Overview of Particulate Matter Measurement Instruments,” *Atmosphere (Basel).*, vol. 6, pp. 1327–1345, 2015.

[10] M. Carminati, L. Pedal, E. Bianchi, F. Nason, G. Dubini, L. Cortelezzi, G. Ferrari, and M. Sampietro, “Capacitive detection of micrometric airborne particulate matter for solid-state personal air quality monitors,” *Sensors Actuators, A Phys.*, vol. 219, pp. 80–87, 2014.

[11] E. Bianchi, E. Rollo, S. Kilchenmann, F. M. Bellati, E. Accastelli, and C. Guiducci, “Detecting particles flowing through interdigitated 3D microelectrodes,” in *Proceedings of the Annual International Conference of the IEEE Engineering in Medicine and Biology Society, EMBS*, 2012, pp. 5002–5005.

[12] B. Giechaskiel, M. Maricq, L. Ntziachristos, C. Dardiotis, X. Wang, H. Axmann, A. Bergmann, and W. Schindler, “Review of motor vehicle particulate emissions sampling and measurement: From smoke and filter mass to particle number,” *J. Aerosol Sci.*, vol. 67, pp. 48–86, 2014.

[13] M. Carminati, L. Pedalà, E. Bianchi, F. Nason, G. Dubini, L. Cortelezzi, G. Ferrari, and M. Sampietro, “Capacitive detection of micrometric airborne particulate matter for solid-state personal air quality monitors,” *Sensors Actuators, A Phys.*, 2014.

[14] Y. Yoshida, Y. Matsuura, T. Inoue, K. Ohtsuka, and Y. Kajiyama, “Metal oxide semiconductor NO2 sensor,” *Sensors Actuators B Chem.*, vol. 25, no. 1–3, pp. 388–391, 1995.

[15] B. Bott and T. A. Jones, “A highly sensitive NO2 sensor based on electrical conductivity changes in phthalocyanine films,” *Sensors and Actuators*, vol. 5, no. 1, pp. 43–53, 1984.

[16] G. Lu, J. Xu, J. Sun, Y. Yu, Y. Zhang, and F. Liu, “UV-enhanced room temperature NO 2 sensor using ZnO nanorods modified with SnO 2 nanoparticles,” *Sensors Actuators, B Chem.*, vol. 162, no. 1, pp. 82–88, 2012.

[17] H. J. Kim and J. H. Lee, “Highly sensitive and selective gas sensors using p-type oxide semiconductors: Overview,” *Sensors Actuators, B Chem.*, vol.

192, pp. 607–627, 2014.

[18] Y. Mun, S. Park, S. An, C. Lee, and H. W. Kim, “NO2 gas sensing properties of Au-functionalized porous ZnO nanosheets enhanced by UV irradiation,” *Ceram. Int.*, vol. 39, no. 8, pp. 8615–8622, 2013.